Catalysis by Hamster Dihydroorotase: Zinc Binding, Site-Directed Mutagenesis, and Interaction with Inhibitors†

Neal K. Williams,‡ Michael K. Manthey,‡ Trevor W. Hambley,§ Séan I. O'Donoghue,|| Mitchell Keegan,‡ Bogdan E. Chapman,‡ and Richard I. Christopherson*,‡

Departments of Biochemistry and Inorganic Chemistry, University of Sydney, Sydney NSW 2006, Australia, and EMBL, Heidelberg D-69012, Germany

Received April 24, 1995; Revised Manuscript Received June 19, 1995⊗

ABSTRACT: Hamster dihydroorotase is the central domain of a trifunctional protein which has been cloned, overexpressed, and purified from *Escherichia coli.* Using the cDNA encoding the dihydroorotase domain, site-directed mutagenesis of amino acid residues conserved between species has enabled identification of three ligands of zinc at the catalytic site as His15, 17 and 158. The underlined amino acids of the nonapeptide sequence Ile12-Asp13-Val14-His15-Val16-His17-Leu18-Arg19-Glu20 from hamster are conserved between dihydroorotases from 8 species. It is proposed that the residues Asp13−His15→Zn^{II} form a triad at the active site and that Arg19, for which even the conservative mutation Arg19→Lys yields an inactive enzyme, is involved in substrate binding. Site-directed mutagenesis of the conserved His186→Ala yielded a mutant enzyme with a reduced affinity for $^{65}Zn^{2+}$. The K_m for dihydroorotate (DHO) increased from 4.0 to 11 μM, while the V_{max} decreased from 1.2 to 0.53 μmol min^{-1} (mg of protein)$^{-1}$, implicating this residue in only a minor way with binding of DHO and in catalysis. The mutation Asp230→Glu resulted in a 14-fold increase in K_m and a 16-fold decrease in V_{max}, indicating involvement of this conserved residue in both binding and catalysis. The mutation Lys239→Gly increased the K_m for DHO 110-fold with a 2-fold increase in V_{max}, suggesting that this residue may form a hydrogen bond with the substrate. The three-dimensional structures of the methyl esters of the substrates *N*-carbamyl-L-aspartate and L-DHO, and the inhibitors, L-6-thiodihydroorotate (TDHO), 2-oxo-1,2,3,6-tetrahydropyrimidine-4,6-dicarboxylate (HDDP), and *trans*- and *cis*-2-oxohexahydropyrimidine-4,6-dicarboxylate (*trans*- and *cis*-HTDP) have already been determined by X-ray crystallography. Correlation of these structures with their affinities for dihydroorotase suggests that DHO binds to the active site with the exocyclic 4-carboxylate group in the axial orientation. ^{1}H NMR spectroscopy indicates that the axial conformations of DHO and TDHO predominate in aqueous solution. Aided by molecular modeling of the portion of the active site formed by the conserved nonapeptide, roles for amino acid residues in substrate binding and catalysis by dihydroorotase are proposed.

The *de novo* biosynthesis of pyrimidine nucleotides is initiated by a trifunctional protein, called CAD or DHO[1] synthetase, which contains the first three enzymic activities of the pathway in the sequence H_3N^+-CPSase-DHOase-bridge-ATCase-COO^- (Jones, 1980; Simmer et al., 1990; Williams et al., 1990). Chemical modification of murine dihydroorotase with diethylpyrocarbonate strongly suggested that there were histidine residues at the active site (Christopherson & Jones, 1979), and time-dependent inactivation with L-cysteine and analogs suggested that there was also a bound zinc atom (Christopherson & Jones, 1980) as has been found for the enzymes from *Clostridium oroticum* (Taylor et al., 1976) and *Escherichia coli* (Washabaugh & Collins, 1984). Christopherson and Jones (1980) proposed that, in the transition state for the reaction catalyzed by dihydroorotase, the two tetrahedral oxygen atoms at C6 are stabilized by formation of an inner sphere coordination complex with the zinc bound at the active site as had been proposed by Walsh (1979) for the bacterial enzyme. Kelly et al. (1986) demonstrated directly the presence of bound zinc on the purified dihydroorotase domain, isolated after digestion of DHO synthetase with elastase.

Several inhibitors of dihydroorotase have been synthesised (Christopherson et al., 1987, 1989; Adams et al., 1988). 6-L-Thiodihydroorotate (TDHO) binds as a competitive inhibitor of dihydroorotase (K_i = 0.85 μM), with the thioxo substituent at C6 likely to form a strong coordination bond with the zinc atom at the active site (Christopherson et al., 1989). 2-Oxo-1,2,3,6-tetrahydropyrimidine-4,6-dicarboxylate (HDDP) is also a competitive inhibitor (K_i = 0.74 μM) and may be considered as a transition-state analog, retaining the two oxygen atoms with a negative charge at C6 (Christopherson

† This investigation received financial support from the University of Sydney Cancer Research Fund and UNDP/World Bank/WHO Special Programme for Research and Training in Tropical Diseases *Corresponding author. Telephone: 61-2-51-6031. Fax: 61-2-351-4726. E-mail: r.christopherson@biochem.usyd.edu.au.

‡ Department of Biochemistry, University of Sydney.

§ Department of Inorganic Chemistry, University of Sydney.

|| EMBL.

⊗ Abstract published in *Advance ACS Abstracts,* August 1, 1995.

[1] Abbreviations: CA-asp, *N*-carbamyl-L-aspartate; DHO, L-dihydroorotate; DHO synthetase, the trifunctional protein containing carbamyl phosphate synthetase (EC 2.7.2.9), aspartate transcarbamylase (EC 2.1.3.2), and dihydroorotase (EC 3.5.2.3); DHO‡, the proposed transition state for the reaction catalyzed by dihydroorotase where there are two oxygen atoms disposed tetrahedrally at C6 of the dihydropyrimidine ring with one negative charge; HDDP, 2-oxo-1,2,3,6-tetrahydropyrimidine-4,6-dicarboxylate; HTDP, 2-oxohexahydropyrimidine-4,6-dicarboxylate; IPTG, isopropyl β-D-thiogalactoside; TDHO, (4*R*)-2-oxo-6-thioxohexahydropyrimidine-4-carboxylate, or L-6-thiodihydroorotate.

0006-2960/95/0434-11344$09.00/0

et al., 1989). TDHO, as the free acid or methyl ester, and HDDP as the dimethyl ester inhibit the growth of human CCRF-CEM leukaemia cells in culture with IC_{50} values of approximately 30 μM (Brooke et al., 1990). The methyl ester of TDHO is toxic to the malarial parasite, *Plasmodium falciparum*, growing in erythrocytic culture with an IC_{50} value of approximately 35 μM (Seymour et al., 1994). The methyl ester and free acid of TDHO have similar effects upon *P. falciparum*, inducing a large accumulation of CA-asp and a decrease of total pyrimidine nucleotides to 57%, consistent with inhibition of malarial dihydroorotase.

While inhibitors of human dihydroorotase are still of some interest as potential anticancer drugs, their use as antimalarial drugs has greater potential, as the malarial parasite, in contrast to humans, is unable to salvage uridine as a precursor of pyrimidine nucleotides (Scheibel & Sherman, 1988). A "second generation" of dihydroorotase inhibitors with greater potency could be designed from a detailed understanding of the basic catalytic mechanism of the enzyme and subtle differences between trifunctional mammalian dihydroorotase and the monofunctional malarial enzyme. We have cloned, overexpressed, and purified the hamster dihydroorotase domain from *E. coli* (Williams et al., 1993), and a similar path is being followed with the malarial enzyme. In this paper, we describe the use of site-directed mutagenesis to determine the roles of certain amino acid residues which have been conserved between dihydroorotases from eight species. This information has been combined with analysis of the conformations of substrates and inhibitors of dihydroorotase to gain an overall picture of the mechanism of catalysis.

EXPERIMENTAL PROCEDURES

Materials and Methods. L-Dihydroorotic acid (DHO), L-aspartate, isopropyl β-D-thiogalactoside (IPTG), Lawesson's reagent, zinc powder, and 4,6-dimethyl-2-hydroxypyrimidine were from Sigma−Aldrich (Castle Hill, Australia). Sodium [^{14}C]bicarbonate (55 Ci/mol) and [^{65}Zn]zinc chloride, carrier-free, were from Amersham International plc (Amersham, U.K.). L-[^{14}C]dihydroorotate was synthesized from [^{14}C]bicarbonate using purified trifunctional DHO synthetase (Christopherson et al., 1989), and *cis*- and *trans*-2-oxohexahydropyrimidine-4,6-dicarboxylic acid (*cis*- and *trans*-HTDP) were also prepared as previously described (Christopherson et al., 1989).

Analysis of Dihydropyrimidine Analogs by ^{1}H NMR Spectroscopy. The purity, chemical structures, and conformations of particular analogs were determined by ^{1}H NMR spectroscopy using Bruker AMX 400- or 600-MHz Fourier transform spectrometers. Chemical shifts are reported in parts per million (δ) relative to an internal reference of acetone (for D_2O) or the residual proton in d_6-DMSO (for d_6-DMSO). For comparitive purposes, the DHO used as a precursor for the synthesis of some analogs was analyzed by ^{1}H NMR (D_2O): δ 2.72 (dd, 1H, J = 5.7, 17.2 Hz, 5-*pro*-*R*-H), 2.90 (dd, 1H, J = 7.0, 17.2 Hz, 5-*pro*-*S*-H), 4.27 (dd, 1H, J = 5.7, 7.0 Hz, H4); (d_6-DMSO): δ 2.54 (dd, 1H, J = 2.5, 16.8 Hz, 5-*pro*-*R*-H), 2.87 (dd, 1H, J = 7.4, 16.8 Hz, 5-*pro*-*S*-H), 4.05 (ddd, 1H, J = 2.5, 4.2, 7.4 Hz, H4), 7.76 (brs, 1H, NH), 10.08 (brs, 1H, NH), 13.1 (brs, 1H, COOH).

DHO Methyl Ester. DHO (920 mg, 5.8 mmol) was dissolved in dry methanol (100 mL). The solution was bubbled with HCl gas for 15 min and then refluxed for 90 min. The reaction mixture was evaporated to dryness, and DHO methyl ester (310 mg, 1.82 mmol) was obtained as white crystals after recrystallization from acetone. ^{1}H NMR (d_6-DMSO): δ 2.56 (dd, 1H, J = 2.5, 16.9 Hz, 5-*pro*-*R*-H), 2.91 (dd, 1H, J = 7.4, 16.9 Hz, 5-*pro*-*S*-H), 3.66 (s, 3H, $COOCH_3$) 4.21 (ddd, 1H, J = 2.5, 4.4, 7.4 Hz, H4), 7.90 (brs, 1H, NH), 10.15 (brs, 1H, NH).

TDHO Methyl Ester. DHO methyl ester (310 mg, 1.8 mmol) was dissolved in dry tetrahydrofuran (35 mL), Lawesson's reagent (445 mg, 1.10 mmol) was added and the mixture was stirred for 16 h at room temperature. The mixture was evaporated to dryness, and the residue was purified on a silica column eluted with benzene, benzene/ether (1:1, v/v), and then ether. The yellow product eluting with ether was evaporated to dryness and then crystallized from chloroform to yield methyl L-6-thiodihydroorotate (156 mg, 0.83 mmol). ^{1}H NMR (d_6-DMSO): δ 3.12 (dd, 1H, J = 2.6, 17.6 Hz, 5-*pro*-*R*-H), 3.25 (dd, 1H, J = 7.2, 17.6 Hz, 5-*pro*-*S*-H), 3.67 (s, 3H, OCH_3), 4.22 (ddd, 1H, J = 2.6, 4.2, 7.2 Hz, H4), 8.59 (brs, 1H, NH), 11.87 (brs, 1H, NH).

TDHO Free Acid. TDHO methyl ester (86 mg, 0.48 mmol) was dissolved in dry tetrahydrofuran (15 ml) and then cooled to 0 °C. Cold deionized water (6 mL) was added, and then LiOH (11 mg, 0.55 mmol), and the mixture was stirred for 3 h at 0 °C. The pH of the solution was adjusted to 3 with Dowex 50WX8-H^+, and the yellow solution was filtered and lyophilized. The residue was redissolved in methanol, the solution was filtered, and L-6-thiodihydroorotic acid was crystallized. ^{1}H NMR (D_2O): δ 2.90 (dd, 1H, J = 5.0, 7.0 Hz, 5-*pro*-*R*-H), 3.08 (dd, 1H, J = 7.0, 17.3 Hz, 5-*pro*-*S*-H), 4.27 (dd, 1H, J = 5.1, 7.1 Hz, H4). d_6-DMSO): δ 3.11 (dd, 1H, J =2.5, 17.4 Hz, 5-*pro*-*R*-H), 3.21 (dd, 1H, J = 7.1, 17.4 Hz, 5-*pro*-*S*-H), 4.05 (ddd, 1H, J = 2.5, 4.6, 7.1 Hz, H4), 8.14 (brs, 1H, NH), 11.80 (brs, 1H, NH), 13.2 (brs, 1H, COOH).

HDDP Dimethyl Ester. 4,6-Dimethyl-2-hydroxypyrimidine (9.92 g, 80 mmol) was dissolved in NaOH (2.5 M, 100 mL) and heated to 70 °C. A solution of $KMnO_4$ (53.7 g, 340 mmol) in water (360 mL, 70 °C) was added dropwise over 2 h, and the mixture was stirred for 2 h at 70 °C, cooled, and filtered. The filtrate was concentrated under vacuum, and cold HCl (10 M, 35 mL) was added to the concentrate at 5 °C until the pH had fallen to 2−3. The resulting precipitate of 2-hydroxypyrimidine-4,6-dicarboxylic acid (6.57 g, 35.7 mmol) was recrystallized from water and after drying was refluxed with acetyl chloride (5.60 g, 71.4 mmol) in dry methanol (350 mL) for 2 h. The solvent was removed, and the crude dimethyl 2-hydroxypyrimidine-4,6-dicarboxylate (3.86 g, 17.7 mmol) was recrystallized from methanol. This compound (1.02 g, 4.7 mmol) was dissolved in glacial acetic acid (70 mL) and heated to 70 °C, and zinc dust (1.50 g, 22.9 mmol) was added over 1 h until a purple color persisted. The mixture was stirred at 70 °C for 30 min and filtered, and the filtrate was evaporated to dryness. The residual colorless oil was dissolved in chloroform (100 mL) and filtered, and the solvent was evaporated to give colorless crystals of dimethyl 2-oxo-1,2,3,6-tetrahydropyrimidine-4,6-dicarboxylate (290 mg, 1.3 mmol), which could be purified by recrystallization from methanol. ^{1}H NMR (d_6-DMSO): δ 3.71 (s, 3H, $COOCH_3$), 3.77 (s, 3H, $COOCH_3$), 4.74 (dd, 1H, J = 2.2, 5.2 Hz, H6), 5.78 (d, 1H, J = 5.2 Hz, H5), 7.18 (brs, 1H, NH), 8.18 (brs, 1H, NH).

Table 1: Mutagenic Oligonucleotides[a]

oligonucleotide	sequence
M-1	192 GGGTTGATCaACGTCCATG 210
M-2	192 GGGTTGATCGACGTtggTGTGCACCTTCGGG 222
M-3	192 GGGTTGATCGACGTtCATGTGggCCTTCGGGAGCCAGG 229
M-4	203 CGTCCATGTGCAtCTTgGGGAGCCAGGTG 231
M-5	203 CGTCCATGTGCAttTaaaGGAGCCAGGTGGG 233
M-6	551 CCCCATTGTGGCagcTGCAGAGCGGC 576
M-7	621 CCAGTGCACATATGTgctGTGGCgCGcAAGGAAGAGATC 659
M-8	703 GTGAGGTCGCACCgCAtgcCCTCTTCCTGAATC 735
M-9	831 GTCATCGACTGCTTcGCgagcaACCACGCTCCCC 864
M-10	831 GTCATCGACTGCTTcGCgagcGAaCACGCTCCCCAT 866
M-11	852 GACCACGCTCCCgcTACCCTcGAGGAGAAGTG 883
M-12	860 TCCCCATACCCTcGAGGAGcgGTGTGGGCCCAA 892
M-13	864 CATACCCTGGAGGAGggGTGTGGtCCCAAGCCTCCACCC 902
M-14	1052 GGATCTGGAGCATGcGTGGACAATCCC 1078

[a] Sequences are presented in the 5′→3′ direction and are numbered according to Figure 1 in Williams et al. (1990). Lowercase letters indicate nucleotide alterations.

HDDP Free Acid. 2-Hydroxypyrimidine-4,6-dicarboxylic acid (240 mg, 1.3 mmol) was dissolved in glacial acetic acid (60 mL) at 70 °C. Zinc dust (600 mg, 9.2 mmol) was added over 30 min, and the reaction was maintained at 70 °C for a further 60 min. The mixture was cooled to room temperature, oxalic acid (200 mg, 2.2 mmol) in acetic acid (10 mL) was added, and after standing for 5 h, the mixture was filtered. The filtrate was evaporated to dryness, and the residue was dissolved in hot water (5 ml), filtered, and cooled to 4 °C for 4 days. The resulting precipitate of 2-oxo-1,2,3,6-tetrahydropyrimidine-4,6-dicarboxylic acid was obtained as off-white crystals (58 mg, 0.31 mmol). Note that HDDP free acid may also be obtained by hydrolysis of the dimethyl ester in 0.1 M NaOH in 90% (v/v) methanol. ^{1}H NMR (d_6-DMSO): δ 4.56 (dd, 1H, J = 2.1, 5.1 Hz, H6), 5.67 (d, 1H, J = 5.1 Hz, H5), 6.99 (brs, 1H, NH), 7.76 (brs, 1H, NH), 12.20 (brs, 1H, COOH).

Strains and Plasmids. The *E. coli* strains used in this work were XL1-Blue (*supE44, hsdR17, recA1, endA1, gyrA96, thi, relA1, lac*$^-$, *F′ [proAB*$^+$, *lacI*^{q} *LacZ*ΔM15, Tn*10(tet*^{r})]), purchased from Stratagene; TG1 (*supE, hsd*Δ5, thi, Δ(lac-proAB), F^1[*traD36, proAB*$^+$, *lacI*^{q}, *lacZ*ΔM15]) from Amersham; and SØ1263 (*araD139,* Δ(lac)U169, rpsL, thi, pyrC), a gift from Dr. Jan Neuhardt (University Institute of Biological Chemistry, Copenhagen, Denmark). The plasmids pCW6-3, pCW6-4 and pCW6-7 and the expression vector pCW12 have been described (Williams et al., 1993).

Plasmid Construction. Oligonucleotides used in the mutagenesis of recombinant plasmids (Table 1) were designed to create or destroy a restriction site while incorporating the desired codon alterations (Table 2) and were synthesized using an Applied Biosystems 381A DNA synthesizer. DNA sequencing of the entire dihydroorotase-encoding region in the mutated products was performed to confirm that only the intended nucleotide changes had occurred. Derivatives of the plasmid pCW6 (Williams et al., 1993) were used as templates for the mutagenesis procedure. Expression plasmids were then constructed by ligating the 1.1-kb *Sca*I−*Hin*dIII fragments from the mutated cDNA vectors (pCW6 derivatives) with pCW12, which had been cut with *Nco*I, blunted with the Klenow fragment, and further digested with *Hin*dIII.

Molecular Modeling of a Conserved Nonapeptide of Dihydroorotase, the Transition State and cis-HTDP. The coordinates of a nonapeptide from residues Ile91 to Ser99, His119, and the zinc atom from the crystal structure of human carbonic anhydrase II (in the Brookhaven Protein Databank; Eriksson et al., 1988a) provided the basis for modeling a portion of the dihydroorotase substrate binding site. Insight II (Biosym Inc., San Diego, CA) was used to convert the conserved nonapeptide of carbonic anhydrase to that of dihydroorotase and for minor structural changes. All subsequent modeling was performed in X-PLOR (Brunger, 1993) using the X-PLOR param19x.pro and toph19x.pro files. Structures were viewed using Midas Plus (Ferrin et al., 1988). Starting models for the three-dimensional structures of the transition state and *cis*-HTDP were derived from the crystal structure of *trans*-HTDP (Hambley et al., 1993). Appropriate substitutions were made to the structure of *trans*-HTDP, and energy minimization was performed as previously described (Hambley et al., 1993).

Table 2: Expression Plasmid Derivatives of cDNA Vectors Modified by Site-Directed Mutagenesis[a]

plasmid derivative	oligonucleotide	new restriction site[b]
pCW23(D230G)	*c*	
pCW27(D13N)	M-1	Δ*Aat*II
pCW24(H15G)	M-2	Δ*Aat*II
pCW24(H17G)	M-3	Δ*Aat*II
pCW27(R19G)	M-4	Δ*Sno*I
pCW27(R19K)	M-5	*Dra*I
pCW27(H134A)	M-6	*Pvu*II
pCW27(H158A)	M-7	*Bss*HII
pCW27(H186A)	M-8	*Sph*HI
pCW27(D230N)	M-9	*Nru*I
pCW27(D230E)	M-10	*Nru*I
pCW27(H234A)	M-11	*Xho*I
pCW27(K239R)	M-12	*Xho*I
pCW27(K239G)	M-13	Δ*Apa*I
pCW27(E301A)	M-14	*Sph*I

[a] The plasmids are the product of cloning the cDNA inserts, modified by site-directed mutagenesis, from pCW6 derivatives (Williams et al., 1993) into pCW12. Amino acid resides are numbered from the N-terminal Thr1 residue of recombinant hamster dihydroorotase [Williams et al. (1993); Thr 55, Figure 1, Williams et al. (1990)]. [b] Specified changes in the plasmid restriction pattern were used to screen for mutagenic products. Δ signifies the destruction of the given existing restriction site, rather than the formation of a new site. [c] pCW23(D230G) is derived from a spontaneous mutation identified by DNA sequencing during routine screening of cDNA inserts during this work. A change of nucleotide 853 [Williams et al. (1990), Figure 1] from A to G resulted in the coding change GAC (Asp) to GGC (Gly).

^{65}Zn Labeling of the Recombinant Dihydroorotase Domain and Mutant Enzymes. M9ZB medium (Studier, 1990)

supplemented with 5 μg/mL thiamine, 11 μg/mL uracil, 0.2% (w/v) glucose, and 100 μg/mL ampicillin was inoculated with a fresh single colony of *E. coli* strain SØ1263 *pyrC*$^-$ transformed with the appropriate expression plasmid and incubated with shaking for 10 h at 30 °C. From this culture, 40 μL was added to 1.5 mL of the same medium containing $^{65}ZnCl_2$ (200 nM, 26 kCi/mol) and growth was continued at 37 °C for 1.5 h. Protein expression was induced by addition of IPTG (10 μM), and incubation was continued with shaking at 30 °C for a further 4.5 h. The entire culture was harvested by centrifugation (8500*g*, 5 min, 20 °C).

Native Polyacrylamide Gel Electrophoresis. *E. coli* cultures (1.5 mL) expressing the dihydroorotase domain were harvested, resuspended in enzyme buffer [300 μL; 10% (v/v) glycerol, 20 mM K-Hepes, pH 7.4, 1 mM DTT, and 0.1 mM EDTA], and sonicated (20 W, 4 × 30 s) using a Branson Sonifier (Branson Sonic Power Company, Danbury, CT) with intermittent cooling of the sample on ice, and cellular debris was removed by centrifugation (8500*g*, 10 min, 4 °C). To the supernatant was added 1 vol of cold, 2× sample buffer [125 mM Tris-HCl pH 6.8, 20% (v/v) glycerol, and 0.2% (w/v) bromophenol blue], and samples were stored on ice prior to electrophoresis. Proteins were separated by polyacrylamide gel electrophoresis using the discontinuous buffer system of Laemmli (1970). Gels were 1.5 mm thick and contained 4% (w/v) acrylamide in the stacking gel and 10% (w/v) acrylamide in the resolving gel. Samples (35 μL) were loaded and electrophoresis was performed at 35 mA (per gel) and constant current (200 V maximum) for approximately 45 min with cooling. The running buffer was 192 mM glycine and 25 mM Tris (pH 8.3). For visualizing ^{65}Zn-labeled proteins, gels were soaked in phosphate-buffered saline plus 3% (v/v) glycerol for 3 h with gentle agitation, dried onto filter paper under vacuum with heating (50 °C) and autoradiographed overnight using Kodak X-ray film. Gels to be stained for proteins were rinsed with 50 mL of destain [10% (v/v) glacial acetic acid and 20% (v/v) methanol] for 30 s with gentle shaking and stained in 0.125% (w/v) Coomassie Blue R-250, 10% (v/v) glacial acetic acid, and 50% (v/v) methanol for approximately 1 h. Gels were destained for approximately 2 h in 2 × 100 mL of destain.

Small-scale Purification and Assay of Dihydroorotase. Recombinant dihydroorotase and mutant forms of the enzyme were purified using a small-scale modification of the procedure of Williams et al. (1993). Kinetic constants of "wild-type" and recombinant dihydroorotases were determined using 10 concentrations of L-[2-^{14}C]DHO ranging from 2 to 100 μM (55.3 Ci/mol) or from 10 to 500 μM (11.1 Ci/mol) for high-K_m mutants. Purified dihydroorotases or crude cell lysates were diluted in enzyme buffer plus $ZnCl_2$ (0.1 mM), and samples (2 μL) were assayed for dihydroorotase activity as described by Christopherson et al. (1989). Reaction velocities were determined by linear regression from three samples taken at 5-min intervals, and K_m and V_{max} values were calculated by nonlinear regression to the Michaelis−Menten equation using the program DNRP53 (Duggleby, 1984). Protein concentrations of enzyme samples were measured at five dilutions by the method of Bradford (1976) and determined by linear regression.

RESULTS

Conformational Analysis of DHO, TDHO, and their Esters by ^{1}H NMR Spectroscopy. Previous analyses of the conformation of DHO and its methyl ester by Katritzky et al. (1969) have shown that each exists in a half-chair conformation with the carboxyl group at C4 preferring the axial orientation. These findings were based on a comprehensive analysis of NMR *J* couplings between the H4 and H5 protons of DHO and those of appropriate model systems. Similarly, we have found that the carboxyl and methoxycarbonyl moieties of TDHO and TDHO-Me, respectively, also prefer the axial orientation in d_6-DMSO ($J_{4,5R}$ DHO = 2.5 Hz; c.f. $J_{4,5R}$ TDHO = 2.5 Hz and $J_{4,5R}$ TDHO-Me = 2.6 Hz). Assuming a lower limit for $J_{4,5R}$ of 2.0 Hz as employed by Katritzky et al. and a negligible influence on this value by replacement of oxygen with sulfur, the experimental $J_{4,5R}$ values for TDHO and TDHO-Me correspond to axial conformer populations of approximately 80% (Katritzky et al., 1969). The lower value limit for $J_{4,5R}$ of 1.9 Hz found for the *tert*-butyl ester of TDHO (C. A. Batty, M. K. Manthey, and R. I. Christopherson, unpublished experiments) indicates that the bulky *tert*-butyloxycarbonyl group is entirely disposed toward the axial orientation. An equatorially disposed alkoxycarbonyl group would be expected to be disfavored due to unfavorable steric interactions with the C5 protons, the preference for an axial orientation increasing with increasing steric bulk (Eliel & Knoeber, 1968).

Due to the poor solubility of the corresponding esters, only the conformations of DHO and TDHO could be determined in aqueous solution. As was the case in DMSO, DHO also prefers the axial orientation in D_2O. The $J_{4,5R}$ coupling constant of 5.7 Hz indicates a time-averaged axial disposition of approximately 60% (Katritzky et al.; 1969, Keys et al., 1985). Similarly, the C4 carboxyl group of TDHO favors the axial configuration in D_2O ($J_{4,5R}$ = 5.0 Hz). These results indicate that, in aqueous solution, the C4 carboxyl groups of DHO and TDHO are predominantly in the axial orientation.

Homology between Dihydroorotases and Other Zinc Enzymes. There are at present eight published dihydroorotase sequences: *E. coli pyrC* (Bäckstrom et al., 1986; Wilson et al., 1987), *Salmonella typhimurium pyrC* (Neuhard et al., 1986), *Saccharomyces cerevisiae URA4* (Guyonvarch et al., 1988), *Ustilago maydis pyr 3* (Spanos et al., 1992), *Bacillus subtilis pyrC* (Quinn et al., 1991), *Dictostelium discoideum PYR1-3* (Faure et al., 1989), *Drosophila melanogaster rudimentary* (Freund & Jarry, 1987), and hamster CAD (Simmer et al., 1990; Williams et al., 1990). All eight amino acid sequences have been aligned (Williams, 1993), revealing only 22 invariant residues. Quinn et al. (1991) performed a similar alignment with all but the *U. maydis* sequence. The limited homology between amino acid sequences of the dihydroorotases is clustered in four regions (Guyonvarch et al., 1988; Williams et al., 1990), suggesting that these fully conserved amino acid residues should play an essential role in zinc or substrate binding, catalysis, or the structure of the enzyme. In order to identify potential zinc ligands in the absence of an X-ray structure for dihydroorotase, sequence homology was sought with zinc enzymes for which the protein crystal structures are known. Figure 1 shows an alignment of the most N-terminal conserved region of the dihydroorotases with a region of the carbonic anhydrases and murine adenosine deaminase. No other sequence similarities were found between dihydroorotases and the known zinc binding sites of other zinc enzymes including carboxypeptidase A, alcohol dehydrogenase, and the zinc

Dihydroorotases										
E. coli	14	D	D	W	H	L	H	L	R	D
S. typhimurium	14	D	D	W	H	V	H	L	R	D
S. cerevisiae	11	C	D	M	H	V	H	V	R	E
U. maydis	12	G	D	F	H	V	H	L	R	Q
B. subtilis	55	V	D	L	H	V	H	F	R	E
D. discoideum	265	V	D	V	H	V	H	L	R	E
D. melanogaster	1486	I	D	V	H	V	H	L	R	S
hamster	12	I	D	V	H	V	H	L	R	E
Carbonic anhydrases					*		*			
Human I	91	F	Q	F	H	F	H	W	G	S
Human II		I	Q	F	H	F	H	W	G	S
Bovine III		R	Q	F	H	L	H	W	G	S
Adenosine Deaminase					*		*			
Mouse	12	V	E	L	H	V	H	L	D	G

FIGURE 1: Comparison of a nine amino acid sequence from a conserved region of the dihydroorotases with nonapeptides of murine adenosine deaminase and three carbonic anhydrases. The crystal structures of the carbonic anhydrases (Kannan et al., 1984; Eriksson et al., 1988a, 1993) as well as murine adenosine deaminase (Wilson et al., 1991) have been determined, and the histidine residues (asterisks) coordinate the active site zinc atoms in these enzymes. The adenosine deaminase sequence is from Yeung et al. (1985), and the carbonic anhydrase sequences are from Vallee and Auld (1990b).

endopeptidases such as thermolysin.

The X-ray structure for carbonic anhydrase shows that the nonapeptide which is homologous to the conserved region of the dihydroorotases (Figure 1) is part of a central β-sheet and contains two of the three His residues that coordinate the zinc atom at the active site (Kannan et al., 1984; Eriksson et al., 1988a; Eriksson & Liljas, 1993). The face of the β-sheet opposite the active site forms part of an extended hydrophobic core of carbonic anhydrase (Eriksson et al., 1988a). The histidyl zinc ligands are adjacent to three large hydrophobic residues, two Phe and a Trp (Figure 1), which participate in the hydrophobic core of carbonic anhydrase (Eriksson et al., 1988a). His94 of carbonic anhydrase is hydrogen-bonded to the amide carbonyl of the Gln92 side chain, forming a "carbonyl−His−zinc triad" (Christianson & Alexander, 1989, 1990). Christianson and Alexander identified this triad, more commonly involving the carboxylate of an Asp residue, in all zinc enzymes with known three-dimensional structures. In adenosine deaminase, the homologous region given in Figure 1 is part of a β-barrel and similarly contains two of the three His residues that coordinate the zinc atom at the active site, located in a deep pocket within the β-barrel (Wilson et al., 1991). In this case, the zinc ligands are adjacent to nonpolar aliphatic residues, two Leu and a Val (Figure 1).

This zinc triad (−C=O···His→Zn^{II}) from the active site of carbonic anhydrase may be found in the homologous conserved regions of the eight dihydroorotases which contain two completely conserved His residues surrounded by hydrophobic residues (Figure 1). Asp13 of hamster dihydroorotase could form a −C=O···His→Zn^{II} triad with His15, in a manner analogous to carbonic anhydrase. The most significant difference between the three groups of sequences is the substitution of Gly98 of the carbonic anhydrases with Asp19 of adenosine deaminase, which accepts hydrogen bonds from substrate analogs bound at the active site (Wilson et al., 1991; Wilson & Quiocho, 1993), and the invariant

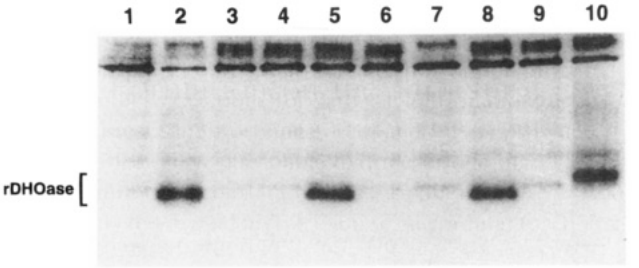

FIGURE 2: Autoradiograph from non-denaturing polyacrylamide gel electrophoresis of proteins from *E. coli* SØ1263 cells grown in the presence of $^{65}Zn^{2+}$. *E. coli* was transformed with the expression plasmids listed. Lane 1, pCW12; lane 2, pCW27; lane 3, pCW24-(H15G); lane 4, pCW24(H17G); lane 5, pCW27(H134A); lane 6, pCW27(H158A); lane 7, pCW27(H186A); lane 8, pCW27(H234A); lane 9, pCW23(D230G); lane 10, pCW27(E301A).

Arg residue of the dihydroorotases which may be involved in the binding of CA-asp or DHO.

Amino Acid Replacements of Potential Zinc Ligands. To identify the zinc binding residues of dihydroorotase, site-directed mutagenesis was used to alter the coding sequence of the cDNA for the recombinant hamster domain. Seven His and acidic residues invariant among the eight known dihydroorotase sequences, and His134, conserved among the dihydroorotase domains of the multifunctional enzymes (Simmer et al., 1990), were substituted with either a Gly or an Ala residue. These amino acids were His15, His17, His134, His158, His186, His234, Asp230, and Glu301. The mutated dihydroorotase sequences were cloned into pCW12, the eight mutant enzymes plus the "wild-type" recombinant dihydroorotase were expressed in *E. coli* grown in the presence of $^{65}ZnCl_2$, and proteins from cell extracts were separated by non-denaturing polyacrylamide gel electrophoresis. An autoradiogram obtained using a PhosphorImager (Molecular Dynamics, Sunnyvale, CA) of the ^{65}Zn-labeled proteins from cell lysates is shown in Figure 2.

In lane 2 of Figure 2, an intense ^{65}Zn-labeled band corresponds with the position for recombinant dihydroorotase, and this band is absent in the extract of cells transformed with the original expression vector pCW12 (lane 1). This ^{65}Zn-labeled band is also evident in lanes 5, 8, and 10, containing the mutants H134A, H234A, and E301A, respectively, showing that these amino acid replacements had no effect on zinc binding. The E301A mutant dihydroorotase migrates more slowly toward the anode than the wild-type protein. In lanes 3, 4, 6 and 9 (H15G, H17G, H158A, and D230G, respectively), no significant ^{65}Zn labeling of the dihydroorotase mutant proteins can be seen, indicating that these amino acid substitutions completely disrupt zinc binding. The mutant protein H186A (Figure 2, lane 7) also lacks zinc binding, although in multiple experiments this mutant commonly displays partial binding of ^{65}Zn, estimated to be 10% of the normal level (data not shown).

Molecular Modeling of Part of the Active Site of Dihydroorotase. On the basis of the sequence homology between carbonic anhydrases and dihydroorotases from various species and the evidence that His15 and His17 residues from the nonapeptide may be involved in zinc binding, part of the active site from hamster dihydroorotase was modeled from the X-ray crystallographic coordinates of residues 91−99 of human carbonic anhydrase II, plus the third zinc ligand, His119, and the zinc atom (Eriksson et al., 1988a). Residues Gln92 and Gly98 of the carbonic anhydrase structure were

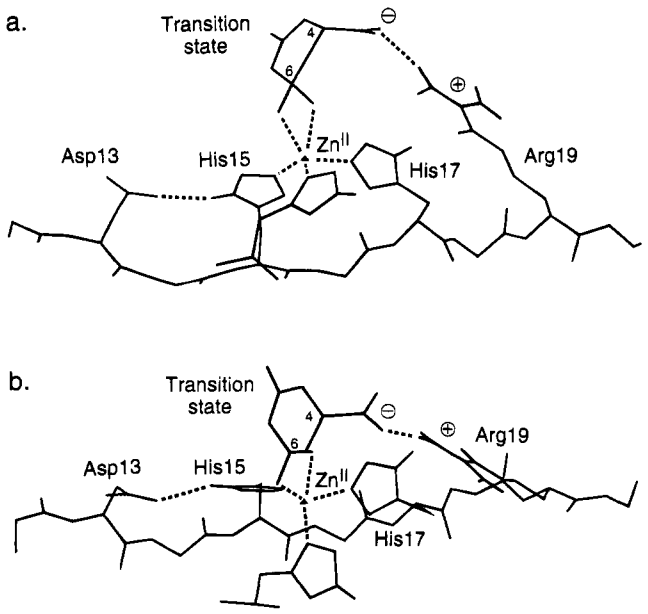

FIGURE 3: Model of a portion of the catalytic site of hamster dihydroorotase based on the structure of a homologous region of human carbonic anhydrase II. The side chains of Asp13, His15, His17, and Arg19, as well as a remote histidine side-chain (in the foreground of panel a), are indicated. All other side chains have been omitted for clarity. DHO‡ and the zinc atom are also shown. Coordination bonds and possible hydrogen and electrostatic bonds are indicated; only amine hydrogens are shown. The minimum distance between the Arg19 side chain and the DHO‡ axial C4 carboxylate is 2.44 Å. Views a and b differ by a rotation of 45° around the horizontal axis in the plane of the page.

replaced with Asp13 and Arg19 of the dihydroorotase sequence using Insight II, and the side chains of the alternating amino acids from the hydrophobic face of the β-sheet (see above) were deleted for clarity. The model represents residues 12−20 of hamster dihydroorotase, -Ile-Asp-Val-His-Val-His-Leu-Arg-Glu-, and includes the bound zinc atom and a third, remote histidyl ligand. A proposed transition state for the reaction (DHO‡) was modeled with tetrahedral oxygens at C6 and an axial 4-carboxylate group based on the crystal structure of DHO-methyl ester (Hambley et al., 1993), to investigate the possible role of Arg19 in substrate binding (Figure 3). For DHO‡, the extra oxygen atom was added at C6 using Insight II, and the positions of the two oxygens were adjusted using energy minimization in X-PLOR, keeping all other atoms fixed. The equatorial conformer of DHO‡ was similarly modeled for comparison, based on the structure of TDHO methyl ester (Hambley et al., 1993). Using X-PLOR, DHO‡ was docked onto the histidine/zinc site of the modeled nonapeptide.

The distances between the two oxygen atoms at C6 and the zinc atom were constrained to 2.15 Å in a multistage docking procedure involving minimal disruption of the carbonic anhydrase coordinates. The final distances between the C4 carboxyl group on DHO‡ and the guanidinium protons of the Arg side chain were 2.44 Å (axial, Figure 3) and 2.14 Å (equatorial, not shown). Initial modeling indicated that, if the nonapeptide of dihydroorotase was part of a β-sheet as observed for carbonic anhydrase, the side chain of Arg19 would be too remote from the proposed catalytic site, centred on the Zn^{2+} ion, to be directly involved in catalysis. Therefore, the distance between the side chain of Arg19 and the carboxylate at C4 of DHO‡ was moved within a distance allowing electrostatic interaction. In the final structure

Table 3: Kinetic Parameters of Recombinant Dihydroorotase and Mutants[a]

dihydroorotase[b]	V_{max} (μmol min^{-1} mg^{-1})	K_m (μM)	V_{mut}/V_{wt}	K_{mut}/K_{wt}
wild type	0.16 ± 0.01	7.1 ± 1.3	1	1
wild type (pure)	1.2 ± 0.1	4.0 ± 0.7	1	1
H186A (pure)	0.53 ± 0.02	11 ± 1	0.44	2.8
D230E	0.010 ± 0.002	99 ± 10	0.063	14
K23R (pure)	1.0 ± 0.02	16 ± 1	0.86	4.0
K239G (pure)	2.4 ± 0.1	450 ± 50	2.0	110
E301A	0.15 ± 0.01	3.5 ± 0.5	0.92	0.49

[a] Dihydroorotase activity was assayed using crude cell lysates or purified enzyme where indicated, with [14C]DHO as substrate. [b] The dihydroorotase mutants D13N, H15G, H17G, R19G, H134A, H158A, D230G, D230N, and H234A had no measurable activity.

(Figure 3), the polypeptide chain is still extended and resembles β-sheet, and the C4 carboxyl of the axial or equatorial conformers of DHO‡ could approach Arg 19, although the resultant orientations of the dihydropyrimidine ring were different. The other modification made to the carbonic anhydrase structure was the replacement of Gln92 with Asp13. The modeled structures show Asp13 of hamster dihydroorotase forming a hydrogen bond with His15 to form a $-C{=}O\cdots His{\rightarrow}Zn^{II}$ triad [see Christianson and Alexander (1989)]. The distance between the carboxyl oxygen of Asp13 and the imidazole hydrogen of His15 was 2.47 Å, within hydrogen-bonding range, although no attempt was made to optimize the geometry.

Substitution of Invariant Amino Acid Residues of Dihydroorotase. The effects of amino acid substitutions of invariant residues on the binding of DHO and subsequent catalysis were determined (Table 3). All mutant dihydroorotase sequences were cloned into pCW12 for protein expression. The D230G, E301A, and six His replacement mutants screened for zinc-binding (Figure 2) were also assayed for dihydroorotase activity. In addition, replacement mutants of Asp13 and Arg19 from the modeled nonapeptide (Figure 1), Lys239, and further mutants of Asp230, were constructed and tested for activity. Some of the mutants with dihydroorotase activity, as well as wild-type recombinant dihydroorotase, were purified on a small scale, and their K_m and V_{max} values were determined. D230E possessed activity but was unstable and could not be purified. The kinetic constants for this mutant, as well as those for E301A, were obtained from crude lysates of induced cultures and compared with a lysate of *E. coli* expressing wild-type recombinant dihydroorotase. A majority of the amino acid substitutions performed (10 of 15) resulted in complete loss of dihydroorotase activity (Table 3). Two inactive dihydroorotase mutants with conservative amino acid replacements, R19K and D230N, were assayed over several ranges of [^{14}C]-DHO concentrations in an attempt to detect low activity.

DISCUSSION

Time-dependent inactivation of murine dihydroorotase by diethylpyrocarbonate (Christopherson & Jones, 1979) and L-cysteine (Christopherson & Jones, 1980) with protection against inactivation by the substrates, CA-asp or DHO, strongly suggested that dihydroorotase contains one or more essential histidine residues and a zinc atom at the active site. In addition, histidines are by far the most common protein ligands in zinc enzymes where the metal ion has a catalytic

function (Vallee & Auld, 1990a). Alignment of the amino acid sequences for dihydroorotases from eight species showed 22 totally conserved residues, of which five were histidines: His15, -17, -158, -186 and -234. Substitution of these histidines (as well as partially conserved His134) with glycine or alanine residues resulted in four mutant dihydroorotases (H15G, H17G, H158A, and H186A) with little or no affinity for ^{65}Zn and two mutants (H134A and H234A) where binding of ^{65}Zn was equivalent to that of wild-type dihydroorotase (Figure 2). His186 has been dismissed as a direct zinc ligand, as H186A commonly displays partial zinc binding (not shown), and has significant catalytic activity, with only moderately altered kinetic parameters (Table 3). These data indicate that histidines 15, 17, and 158 are likely to be zinc ligands at the active site of the hamster dihydroorotase domain, but His186 cannot be excluded as an additional zinc ligand. Brown and Collins (1991) have proposed that histidines 17 and 19 from the conserved nonapeptide of *E. coli* dihydroorotase are zinc ligands. They found some evidence for a thiolate ligand and a pentacoordinated zinc. It was noted, however, that no cysteines are conserved throughout the known dihydroorotase sequences, and that catalytic zinc atoms rarely contain sulfur ligands in their coordination sphere (Vallee & Auld, 1990b). The homologous zinc ligands for carbonic anhydrase are histidines 94, 96, and 119, and those for murine adenosine deaminase and histidines 15, 17 and 214 (Figure 1).

These zinc enzymes each contain a conserved nonapeptide with likely $-C{=}O\cdots His{\rightarrow}Zn^{II}$ triads (Christianson & Alexander, 1989) and a remote third histidyl residue acting as zinc ligands. The reactions catalyzed by dihydroorotase, carbonic anhydrase, and adenosine deaminase are also chemically similar where hydrolysis of DHO $\rightarrow$ CA-asp, hydration of $CO_2 \rightarrow HCO_3^-$, and deamination of (deoxy)-adenosine $\rightarrow$ (deoxy)inosine are likely to be initiated by OH^- formed by ionization of a zinc-bound water molecule at the active site. The polarized carbonyl of the substrate would undergo nucleophilic attack by the zinc-bound OH^-, resulting in a tetrahedral oxyanion transition state, ($DHO^{\ddagger}$), for dihydroorotase and the product, HCO_3^-, for carbonic anhydrase (Eriksson et al., 1988b; Håkansson et al., 1992). In adenosine deaminase, the zinc-activated water or hydroxide attacks the susceptible sp^2-hybridized C6, resulting in a tetrahedral transition state (Wilson & Quiocho, 1993). The pH rate profiles for dihydroorotase indicate the involvement of a catalytic group with a pK_a of 7.1 (Christopherson & Jones, 1979), and the pK_a of the zinc-bound water molecule of carbonic anhydrase is approximately 7 (Steiner et al., 1975; Silverman & Lindskog, 1988; the pK_a of the zinc-bound water molecule of adenosine deaminase has not been reported). The amino acid sequences of these three enzymes are homologous only for their conserved nonapeptides (Figure 1). It would seem likely that this homology arose through convergent evolution due to the similarity of catalytic mechanisms of zinc enzymes.

For carbonic anhydrase, $-C{=}O\cdots His{\rightarrow}Zn^{II}$ triads involve hydrogen bonds between the carbonyl of the amide groups of Gln92 and His94 and Glu117 and His119 (Eriksson et al., 1988a), while for hamster dihydroorotase, a hydrogen bond is proposed between the carboxylate of Asp13 and His15 (Figures 1 and 3). The conservative substitution D13N could still have formed a hydrogen bond between the carbonyl of the amide of the substituted Asn13 and His15,

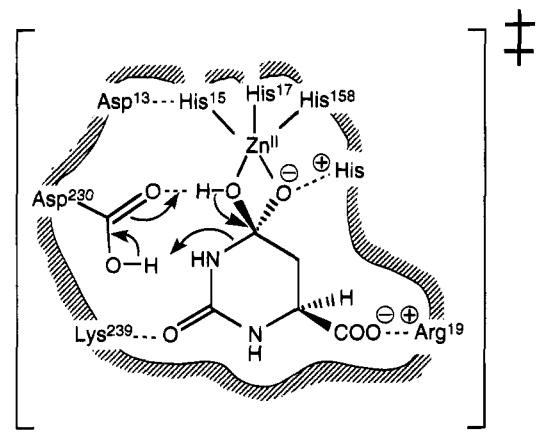

FIGURE 4: The enzyme–transition state complex for hamster dihydroorotase indicating proposed functions for conserved amino acid residues. An unidentified histidine is shown interacting with the negatively charged oxygen at C6 of the tetrahedral intermediate, analogous to the roles of His231 and Arg127 of thermolysin and carboxypeptidase A, respectively. Hydrogen bonds and electrostatic interactions are indicated by dashed lines. Subsequent electronic shifts indicated are for the reverse reaction of DHO hydrolysis.

but this mutant dihydroorotase showed no catalytic activity in the presence of 0.01–10 mM [^{14}C]DHO (Table 3). A hydrogen bond to a negatively charged carboxylate group would have a stronger effect on the Lewis basicity of His15 compared with a hydrogen bond to the carbonyl of an amide. The loss of dihydroorotase activity for the mutant D13N could be due to a decrease in zinc affinity or a change in the pK_a of the bound water molecule. In adenosine deaminase, Asp19 of the conserved nonapeptide (Figure 1) is involved in hydrogen bonding to the 3′ and 5′ hydroxyls of the ribose of adenosine (Wilson & Quiocho, 1993). We have proposed that Arg19 of hamster dihydroorotase forms an electrostatic bond with the C4 carboxylate of DHO (Figure 3) or the equivalent α-carboxylate of CA-asp. It might therefore be predicted that the conservative substitution R19K would yield a mutant enzyme with a decreased affinity or a high K_m for DHO. However, this mutant dihydroorotase showed no catalytic activity (Table 3), suggesting that the proposed electrostatic interaction between Arg19 and the 4-carboxylate of DHO must have a high degree of stereospecificity.

The mutant dihydroorotase D230G did not bind ^{65}Zn (Figure 2), suggesting that Asp230 may interact closely with the zinc at the active site. In adenosine deaminase, the active site residue Asp295 forms a fourth coordination bond to the zinc and is hydrogen-bonded to the zinc-activated water molecule. It was initially proposed that Asp295 acts as a catalytic base, accepting a proton from the activated water (Wilson et al., 1991), although this may be achieved by His238 (Wilson & Quiocho, 1993). For the zinc proteases thermolysin and carboxypeptidase A, the carboxylate groups of Glu143 and Glu270, respectively, act as general bases, initially abstracting a proton from the zinc-coordinated water molecule, and as general acids to donate a proton to the nitrogen of the scissile peptide bond, inducing collapse of the tetrahedral oxyanion transition state (Matthews, 1988; Christianson & Lipscomb, 1989). Similarly for dihydroorotase, Asp230 may hydrogen bond to $Zn^{II}OH_2$. The mutant enzyme, D230G, is catalytically inactive (Table 3) with a reduced affinity for zinc. The mutant D230N is also inactive (Table 3), consistent with the proposed catalytic role of

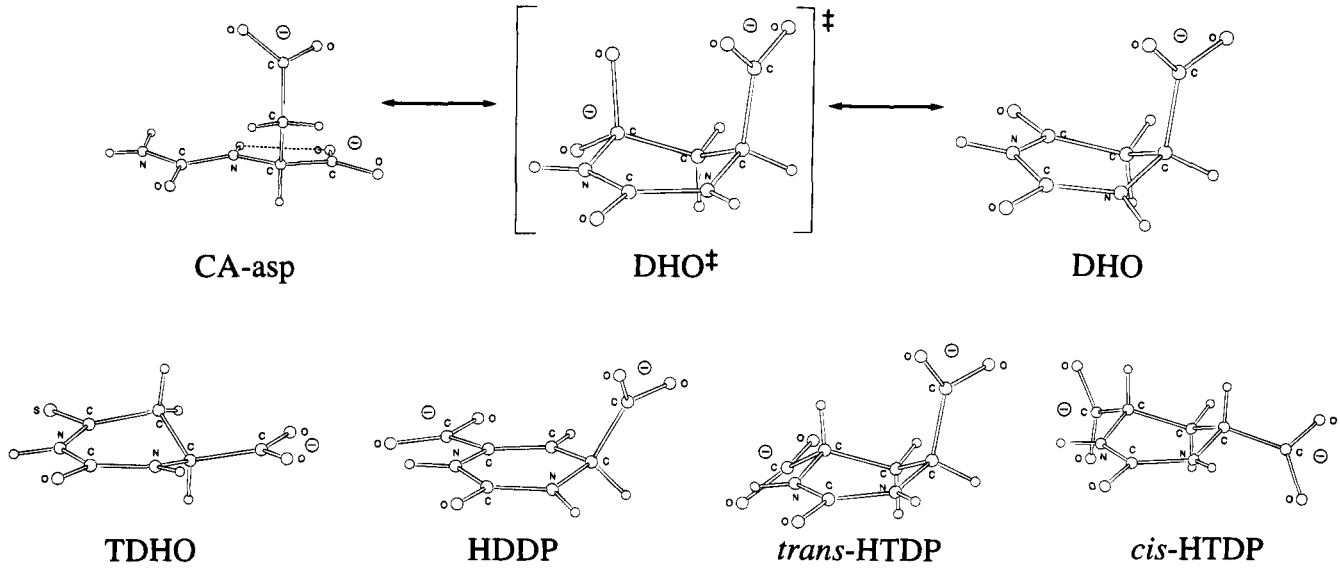

FIGURE 5: Conformational representations of the reaction catalyzed by dihydroorotase and some inhibitors. The three-dimensional structures of CA-asp (Zvargulis et al., 1994), DHO, and inhibitors (Hambley et al., 1993) have been determined by X-ray crystallography. The conformations of the transition state (DHO‡) and *cis*-HTDP were derived from that for *trans*-HTDP as described under Experimental Procedures. Except for CA-asp, the structures of these molecules were determined as methyl esters; these methyl groups have been omitted to indicate the structures which interact with dihydroorotase.

Asp230 as a general acid/base. The conservative mutant D230E has dihydroorotase activity (K_{mut}/K_{wt}= 14; V_{mut}/V_{wt} = 0.063; Table 3), suggesting a role for Asp230 in the binding of DHO and in subsequent catalysis. The mutant enzyme D230E was unstable and could not be purified in active form, suggesting a loss of zinc during purification or some conformational transition. The mutant dihydroorotase H186A also has reduced affinity for zinc (Figure 2) and approximately half the wild-type activity (K_{mut}/K_{wt} = 2.8; V_{mut}/V_{wt} = 0.44; Table 3). Zimmermann et al. (1994) replaced His186 (His 1642 using their numbering system) with Asn and found that the mutant retained some enzymic activity. The relatively moderate effects on K_m and V_{max} for the mutant H186A suggest that His186 may be close to the zinc and bound substrate but may not interact directly.

The mutant H234A is catalytically inactive but binds zinc with an affinity similar to that of the wild-type enzyme (Table 3; Figure 2). Zimmermann et al. (1994) constructed a mutant dihydroorotase with the equivalent of His234 (His1690) substituted with Asn, H234N, which had a 34-fold lower k_{cat} (V_{max}/K_m), a 9-fold higher K_m, and a reduced pH dependence, implicating His234 in substrate binding and in catalysis. Lys239 of the recombinant hamster dihydroorotase domain was replaced with both Arg and Gly with little effect upon V_{max} (Table 3). For K239R, K_{mut}/K_{wt} = 4.0, indicating that this conservative mutation has resulted in a moderate decrease in the affinity of the enzyme for DHO. Loss of the basic side chain for the mutant K239G resulted in a large decrease in DHO affinity; K_{mut}/K_{wt} = 110. Substitution of this ratio into eq 2 (Wells & Fersht, 1985),

$$G = -RT \ln(K_{mut}/K_{wt}) \quad (2)$$

shows that this increase in K_m corresponds to a weakening of the substrate binding energy by 2.9 kcal/mol. This loss of binding energy is consistent with the loss of a hydrogen bond between Lys239 and an uncharged group (Fersht et al., 1985) on DHO, perhaps the ureido carbonyl group at C2. A schematic representation of the enzyme−transition state complex for hamster dihydroorotase is presented in Figure 4, summarizing the proposed functions of the conserved residues investigated in this work. Asp230 is shown hydrogen-bonded to the hydroxyl group of the tetrahedral intermediate formed from the zinc-activated water molecule and acting as the general acid/base in the hydrolysis of DHO → CA-asp.

Christopherson and Jones (1980) used a variety of analogs to show that the α-carboxylate of CA-asp or the 4-carboxylate of DHO is essential for binding to dihydroorotase, and an electrostatic interaction with a positive charge on the enzyme was proposed. Data presented here suggest that the enzyme residue is Arg19. The three-dimensional structures of the methyl esters of DHO, TDHO, HDDP, and *trans*-HTDP have been determined by X-ray crystallography (Hambley et al., 1993). In the crystalline state, the methyl ester of DHO adopts a conformation with the 4-methoxycarbonyl moiety in the axial orientation, while the same group in the methyl ester of TDHO is equatorial (Figure 5). ^{1}H NMR at 600 MHz in D_2O of the free acids of DHO and TDHO shows that the C4 carboxylate groups are predominantly (60%) in the axial conformation in aqueous solution (see Results). The potent inhibitor HDDP (K_i = 0.74 μM; Christopherson et al., 1989) has an equatorial carboxylate at C6, adjacent to the C=C double bond, and an axial carboxylate at C4 (Figure 5). Addition of a further 2 equiv of hydrogen to HDDP yields *cis*-HTDP (Figure 5), which does not inhibit dihydroorotase (Christopherson et al., 1989). Racemization of *cis*-HTDP produced *trans*-HTDP (Figure 5; Christopherson et al., 1989) which bound strongly to dihydroorotase ($K_i \approx$ 12 μM). These observations indicate that DHO is probably bound to dihydroorotase in the axial conformation as indicated for DHO‡ in Figure 5. *cis*-HTDP does not bind to dihydroorotase because when one carboxylate is equatorial, mimicking the two oxygens at C6 of DHO‡, the other carboxylate must also be equatorial. Thus, the carboxylates of *cis*-HTDP must either be equatorial−equatorial or axial−axial, and neither conformer will bind.

By contrast, *trans*-HTDP can adopt equatorial−axial or axial−equatorial conformations, which are equivalent because of an axis of symmetry through the molecule (Figure 5), and both can bind to dihydroorotase in a similar way to HDDP. The chelating inhibitor TDHO (K_i = 0.85 μM; Christopherson et al., 1989) would also bind to dihydroorotase with the 4-carboxylate group in the axial position. The slight preference for the axial configuration of the carboxylate group of DHO and TDHO in aqueous solution as determined by ^{1}H NMR and the small free energy difference between the readily interconvertible axial and equatorial conformers of DHO (Keys et al., 1985) would imply that both compounds have only moderate entropy demands upon binding to dihydroorotase. However, inhibitors of dihydroorotase where the carboxylate group is constrained to the axial orientation could exhibit enhanced binding characteristics.

REFERENCES

Adams, J. L., Meek, T. D., Mong, S.-M., Johnson, R. K., & Metcalf, B. W. (1988) *J. Med. Chem. 31*, 1355−1359.

Bäckstrom, D., Sjöberg, R. M., & Lundberg, L. G. (1986) *Eur. J. Biochem. 160*, 77−82.

Bradford, M. M. (1976) *Anal. Biochem. 72*, 248−254.

Brooke, J., Szabados, E., Lyons, S. D., Goodridge, R. J., Harsanyi, M. C., Poiner, A., & Christopherson, R. I. (1990) *Cancer Res. 50*, 7793−7798.

Brown, D. C., & Collins, K. D. (1991) *J. Biol. Chem. 266*, 1597−1604.

Brunger, A. T. (1993) *X-PLOR Version 3.1: A system for X-ray crystallography and NMR*, Yale University Press, New Haven, CT.

Christianson, D. W., & Alexander, R. S. (1989) *J. Am. Chem. Soc. 111*, 6412−6419.

Christianson, D. W., & Alexander, R. S. (1990) *Nature 346*, 225.

Christianson, D. W., & Lipscomb, W. N. (1989) *Acc. Chem. Res. 22*, 62−69.

Christopherson, R. I., & Jones, M. E. (1979) *J. Biol. Chem. 254*, 12506−12512.

Christopherson, R. I., & Jones, M. E. (1980) *J. Biol. Chem. 255*, 3358−3370.

Christopherson, R. I., Schmalzl, K. J., & Sharma, S. C. (1987) Complete patent specification: Australia 77692/87, Japan 220095/87, U.S. 091 761, South Africa 87/6552, Europe 87307744.0.

Christopherson, R. I., Schmalzl, K. J., Szabados, E., Goodridge, R. J., Harsanyi, M. C., Sant, M. E., Algar, E. M., Anderson, J. E., Armstrong, A., Sharma, S. C., Bubb, W. A., & Lyons, S. D. (1989) *Biochemistry 28*, 463−470.

Duggleby, R. G. (1984) *Comput. Biomed. Res. 14*, 447−455.

Eliel, E. L., & Knoeber, M. C. (1968) *J. Am. Chem. Soc. 90*, 3444−3458.

Eriksson, A. E., & Liljas, A. (1993) *Proteins 16*, 29−42.

Eriksson, A. E., Jones, T. A., & Liljas, A. (1988a) *Proteins 4*, 274−282.

Eriksson, A. E., Kylsten, P. M., Jones, T. A., & Liljas, A. (1988b) *Proteins 4*, 283−293.

Faure, M., Camonis, J. H., & Jacquet, M. (1989) *Eur. J. Biochem. 179*, 345−358.

Ferrin, T. E., Huang, C. C., Jarvis, L. E., & Langridge, R. (1988) *J. Mol. Graphics 6*, 13−27.

Freund, J. N., & Jarry, B. P. (1987) *J. Mol. Biol. 193*, 1−13.

Guyonvarch, A., Nguyen-Juilleret, M., Hubert, J. C., & Lacroute, F. (1988) *Mol. Gen. Genet. 212*, 134−141.

Håkansson, K., Carlsson, M., Svensson, L. A., & Liljas, A. (1992) *J. Mol. Biol. 227*, 1192−1204.

Hambley, T. W., Phillips, L., Poiner, A. C., & Christopherson, R. I. (1993) *Acta Crystallogr. B49*, 130−136.

Jones, M. E. (1980) *Annu. Rev. Biochem. 49*, 253−279.

Kannan, K. K., Ramanadham, M., & Jones, T. A. (1984) *Ann. N.Y. Acad. Sci. 429*, 49−60.

Katritzky, A. R., Nesbit, M. R., Kurtev, B. J., Layapova, M., & Pojarlieff, I. G. (1969) *Tetrahedron 25*, 3807−3824.

Kelly, R. E., Mally, M. I., & Evans, D. R. (1986) *J. Biol. Chem. 261*, 6073−6083.

Keys, L. D., II, & Johnston. M. (1985) *J. Am. Chem. Soc. 107*, 486−492.

Laemmli, U. K. (1970) *Nature 227*, 680−685.

Matthews, B. W. (1988) *Acc. Chem. Res. 21*, 333−340.

Neuhard, J., Kelln, R. A., & Stauning, E. (1986) *Eur. J. Biochem. 157*, 335−342.

Quinn, C. L., Stephenson, B. T., & Switzer, R. L. (1991) *J. Biol. Chem. 266*, 9113−9127.

Scheibel, L. W., & Sherman, I. W. (1988) in *Malaria: Principles and Practice of Malariology* (Wernsdorfer, W. H., & McGregor, I., Eds.) pp 234−242, Churchill Livingstone, Melbourne.

Seymour, K. K., Lyons, S. D., Phillips, L., Rieckmann, K. H., & Christopherson, R. I. (1994) *Biochemistry 33*, 5268−5274.

Silverman, D. N., & Lindskog, S. (1988) *Acc. Chem. Res. 21*, 30−36.

Simmer, J. P., Kelly, R. E., Rinker, A. G., Jr., Zimmermann, B. H., Scully, J. L., Kim, H., & Evans, D. R. (1990) *Proc. Natl. Acad. Sci. U.S.A. 87*, 174−178.

Spanos, A., Kanuga, N., Holden, D. W., & Banks, G. R. (1992) *Gene 117*, 73−79.

Steiner, H., Jonsson, B. H., & Lindskog, S. (1975) *Eur. J. Biochem. 59*, 253−259.

Studier, F. W., Rosenberg, A. H., Dunn, J. J., & Dubendorff, J. W. (1990) *Methods Enzymol. 185*, 60−89.

Taylor, W. H., Taylor, M. L., Balch, W. E., & Gilchrist, P. S. (1976) *J. Bacteriol. 127*, 863−873.

Vallee, B. L., & Auld, D. S. (1990a) *Proc. Natl. Acad. Sci. U.S.A. 87*, 220−224.

Vallee, B. L., & Auld, D. S. (1990b) *Biochemistry 29*, 5647−5659.

Walsh, C. (1979) *Enzymatic Reaction Mechanisms*, p 154, W. H. Freeman and Co., San Francisco.

Washabaugh, M. W., & Collins, K. D. (1984) *J. Biol. Chem. 259*, 3293−3298.

Wells, T. N. C., & Fersht, A. R. (1985) *Nature 316*, 656−657.

Williams, N. K. (1993) Ph.D. Thesis, University of Sydney.

Williams, N. K., Simpson, R. J., Moritz, R. L., Peide, Y., Crofts, L., Minasian, E., Leach, S. J., Wake, R. G., & Christopherson, R. I. (1990) *Gene 94*, 283−288.

Williams, N. K., Peide, Y., Seymour, K. K., Ralston, G. B., & Christopherson, R. I. (1993) *Protein Eng. 6*, 333−340.

Wilson, D. K., & Quiocho, F. A. (1993) *Biochemistry 32*, 1689−1694.

Wilson, D. K., Rudolph, F. B., & Quiocho, F. A. (1991) *Science 252*, 1278−1284.

Wilson, H. R., Chan, P. T., & Turnbough, C. L. (1987) *J. Bacteriol. 169*, 3051−3058.

Yeung, C.-Y., Ingolia, D. E., Roth, D. B., Shoemaker, C., Al-Ubaidi, M. R., Yen, J.-Y., Ching, C., Bobonis, C., Kaufman, R. J., & Kellems, R. E. (1985) *J. Biol. Chem. 260*, 10299−10307.

Zimmermann, B. H., Kemling, N., & Evans, D. R. (1994) In *Purine and Pyrimidine Metabolism in Man VIII* (in press).

Zvargulis, E. S., & Hambley, T. W. (1994) *Acta Crystallogr. C50*, 2058−2060.

BI950908F